

RSC Advances



This is an *Accepted Manuscript*, which has been through the Royal Society of Chemistry peer review process and has been accepted for publication.

Accepted Manuscripts are published online shortly after acceptance, before technical editing, formatting and proof reading. Using this free service, authors can make their results available to the community, in citable form, before we publish the edited article. This *Accepted Manuscript* will be replaced by the edited, formatted and paginated article as soon as this is available.

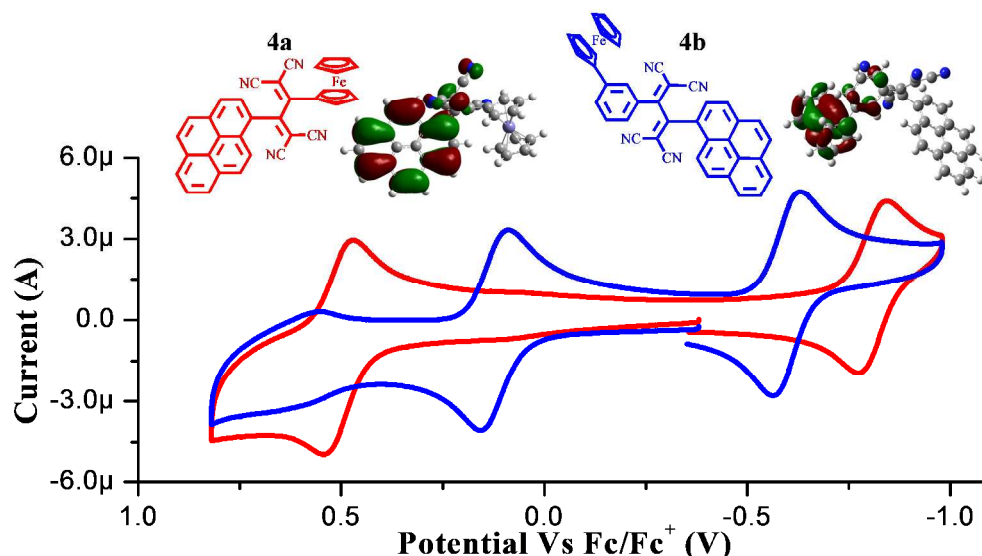
You can find more information about *Accepted Manuscripts* in the [Information for Authors](#).

Please note that technical editing may introduce minor changes to the text and/or graphics, which may alter content. The journal's standard [Terms & Conditions](#) and the [Ethical guidelines](#) still apply. In no event shall the Royal Society of Chemistry be held responsible for any errors or omissions in this *Accepted Manuscript* or any consequences arising from the use of any information it contains.

Synergistic effect of donors on the tetracyanobutadiene (TCBD) substituted ferrocenyl pyrenes

Bhausahab Dhokale, Thaksen Jadhav, Shaikh M. Mobin and Rajneesh Misra*

Department of Chemistry, Indian Institute of Technology Indore 452 017 (India)



ABSTRACT

A set of ferrocenyl substituted pyrenes **2** and **3a** – **3c** were designed and synthesized by the Pd-catalyzed Suzuki and Sonogashira cross-coupling reactions. The [2+2] cycloaddition-retroelectrocyclization reaction of ferrocenyl substituted pyrenes **3a** and **3b** with tetracyanoethylene (TCNE), resulted tetracyanobutadiene (TCBD) derivatives **4a**, and **4b** respectively. The synergistic effects of two donors (ferrocene and pyrene) and TCBD acceptor on their photonic properties, energy levels and donor-acceptor interactions are evaluated. The photophysical and electrochemical properties of **2** and **3a** – **3c** were compared with **4a** and **4b**. The ferrocenyl substituted pyrene **4b** exhibits a strong charge transfer band from pyrene to TCBD and a weak charge transfer band from ferrocene to TCBD, whereas **4a** exhibits two strong charge transfer bands, one from ferrocene to TCBD and another from pyrene to TCBD. The characteristic emission pattern of ferrocenyl substituted pyrenes **2**, **3a** – **c**, **4a** and **4b** indicates the emission from pyrene moiety. The electrochemical properties reveal strong electronic communication

between ferrocene and TCBD in **4a**, and weak electronic communication in **4b**. The experimental observation and conclusion were supported by computational calculations. The single crystal X-ray structure of ferrocenyl substituted pyrene **3b** is reported.

INTRODUCTION

In recent years research on multistate redox active π -conjugated donor-acceptor (D-A) molecular systems has gained momentum due to their wide range of applications in non-linear optics (NLO), photovoltaic systems, light harvesting antenna, energy transfer cassettes, sensors and memory storage devices.¹ The photonic properties of D-A systems can be tuned by slight variations in the nature of donor, acceptor or the spacer unit.² The synergistic effect of multiple donors containing reversible redox active center and an acceptor can further perturbs electronic energy levels of molecule. We were interested to see the synergistic effect of two donors (ferrocene and pyrene) and the TCBD acceptor on photonic properties, energy levels and D-A interactions.

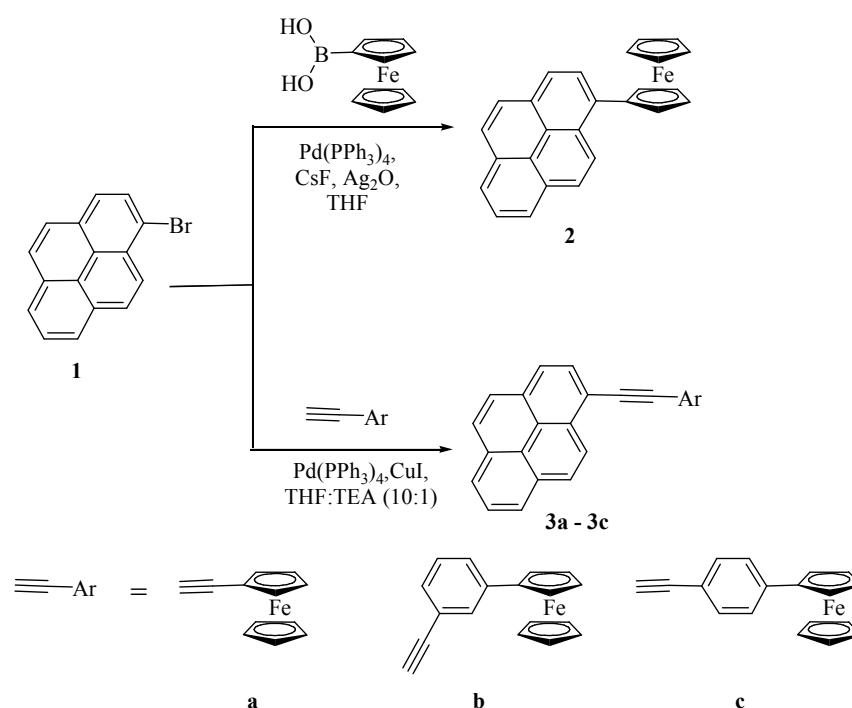
Pyrene is the smallest peri-fused polycyclic aromatic hydrocarbon widely studied for its unique photonic and optoelectronic applications.³ It is a versatile fluorophore and exhibits strong absorption and high fluorescence quantum yield. It is well known donor but can behave as an acceptor, depending on the nature of the attached substituent.⁴

The ferrocene is widely studied metallocene with strong electron donating ability, rich electrochemistry and non-linear optical behavior.⁵ Our group has explored ferrocene as a strong donor and attached to variety of chromophores with varying spacer length.⁶ Pyrene and ferrocene both are strong donors.⁷ There are couple of reports, where ferrocenyl coupled pyrenes are used for sensing and NLO applications.⁸

Diederich *et al.* has explored the [2+2] cycloaddition-retroelectrocyclization reaction of ferrocenyl substituted alkynes with tetracyanoethelene (TCNE), which results in TCBD substituted ferrocenyl derivatives.⁹ The literature reveals that there are no reports on the reaction of alkynylated ferrocenyl pyrenes with TCNE, which will result in unsymmetrical, D-A-D' type molecular system.

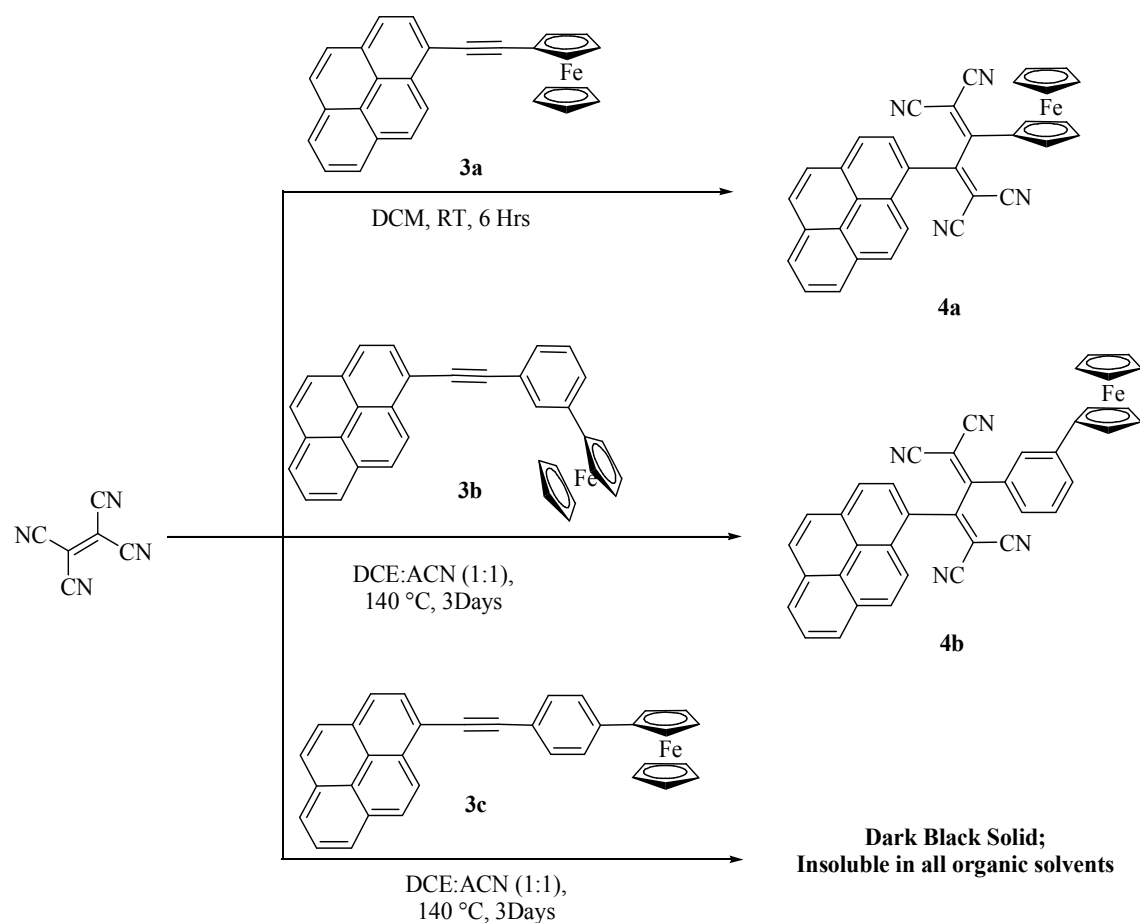
Herein we report the design, synthesis and properties of ferrocenyl substituted pyrenes and their TCBD derivatives. The ferrocenyl substituted pyrenes (**2** and **3a – 3c**) of varying spacer length were synthesized by Suzuki and Sonogashira coupling reactions and the TCBD derivatives **4a** and **4b** were synthesized by [2+2] cycloaddition-retroelectrocyclization reaction. We were interested to see the synergistic effect of two donors (ferrocene and pyrene) and the TCBD acceptor on the photonic properties, energy levels and D-A interactions.

RESULTS AND DISCUSSION



Scheme 1. Synthetic route for the ferrocenyl substituted pyrenes **2** and **3a – 3c**.

The ferrocenyl substituted pyrenes **2** and **3a – 3c** were synthesized by the Pd-catalyzed Sonogashira cross-coupling reactions of 1-bromo pyrene **1** with corresponding ferrocenyl counterparts (Scheme 1). The Suzuki cross-coupling reaction of 1-bromopyrene **1** with ferrocenyl boronic acid resulted ferrocenyl substituted pyrene **2** in 70 % yield, whereas the Sonogashira cross-coupling reaction of 1-bromopyrene **1** with respective ferrocenyl alkynes (**a – c**) resulted **3a – 3c** in 68 %, 70 % and 61 % yields respectively. The ferrocenyl substituted pyrenes were purified by repeated column chromatography and recrystallization.



Scheme 2. Synthetic route for the ferrocenyl substituted pyrenes **4a** and **4b**.

The [2+2] cycloaddition-retroelectrocyclization reaction of ferrocenyl substituted pyrene **3a** with tetracyanoethylene (TCNE) in dichloromethane at room temperature resulted ferrocenyl substituted pyrene **4a** in 80 % yield (Scheme 2). Under similar reaction condition ferrocenyl substituted pyrenes **3b** and **3c** failed to undergo [2+2] cycloaddition-retroelectrocyclization reaction. By increasing the reaction temperature from room temperature to 140 °C, **3b** undergoes [2+2] cycloaddition-retroelectrocyclization reaction with TCNE in mixture of solvents dichloroethane and acetonitrile (DCE:ACN) (1:1) and resulted **4b** in 85 % yield. Under similar reaction condition ferrocenyl substituted pyrene **3c** resulted dark black solid, which was insoluble in common organic solvents. The ferrocenyl substituted pyrenes were well characterized by usual spectroscopic techniques. The **3b** was also characterized by single crystal X-ray crystallography.

PHOTOPHYSICAL PROPERTIES

The color of ferrocenyl substituted pyrenes **2**, **3a – 3c**, **4a** and **4b** in dichloromethane solution in day light are displayed in Figure S1 (ESI). The ferrocenyl substituted pyrenes **3a** and **3c** exhibit intense yellow color compared to **2** and **3b**. The ferrocenyl substituted pyrene **4a** exhibits dark gray color due to the presence of two strong charge transfer interactions (from ferrocene to TCBD; pyrene to TCBD) whereas the ferrocenyl substituted pyrene **4b** exhibits dark brown color due to single strong charge transfer interaction (from pyrene to TCBD) and weak a charge transfer interaction (from ferrocene to TCBD).

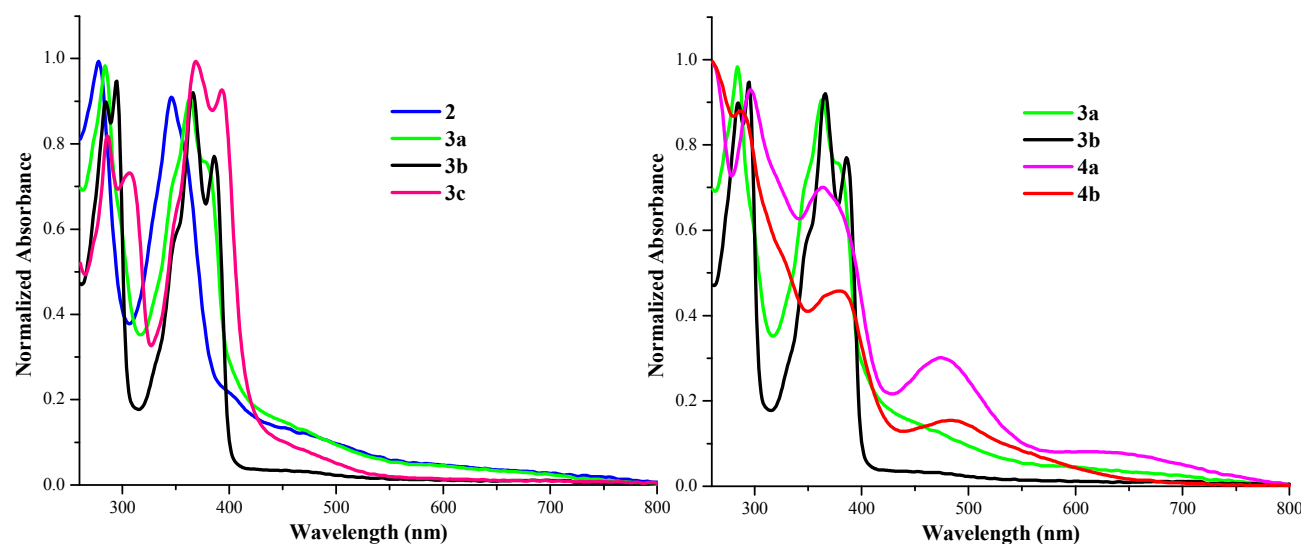


Figure 1. Normalized electronic absorption spectra of ferrocenyl substituted pyrenes **2**, **3a – 3c**, **4a** and **4b** in dichloromethane.

The absorption spectra of ferrocenyl substituted pyrenes **2**, **3a – 3c**, **4a** and **4b** were recorded in dichloromethane and are displayed in Figure 1. The $S_0 \rightarrow S_1$ and $S_0 \rightarrow S_2$ absorption bands appear in the regions ~ 360 nm and ~ 280 nm respectively (Table 1). The successive red shift in the $S_0 \rightarrow S_1$ and $S_0 \rightarrow S_2$ absorption bands of ferrocenyl substituted pyrenes **2**, and **3a – 3c** follows the order $3c > 3b > 3a > 2$.

The absorption spectra of ferrocenyl substituted pyrenes **2** and **3a – 3c**, show characteristic vibronic pattern of pyrene, on the other hand the characteristic vibronic pattern is disappeared in the absorption spectra of **4a** and **4b**, indicating strong interaction of the pyrene with TCBD. The ferrocenyl

substituted pyrenes **4a** and **4b** exhibit strong charge transfer bands at 474 nm and 483 nm respectively corresponding to the charge transfer from pyrene to TCBD moiety. The red shifted CT band in **4b** than **4a** indicates stronger D-A interaction between pyrene and TCBD in **4b**. The strong absorption band at 639 nm in **4a** corresponds to the charge transfer from ferrocene to TCBD,¹⁰ indicating stronger D-A interaction between ferrocene and TCBD in **4a**. The small shoulder at lower energy region to the absorption at 483 nm in **4b** may be assigned to the weak charge transfer from ferrocene to the TCBD indicating weaker D-A interaction between ferrocene and TCBD due to the *meta* linkage.

Table 1. Photophysical properties of ferrocenyl substituted pyrenes **2**, **3a – 3c**, **4a** and **4b**.

	λ_{\max} (nm)	$\epsilon/10^4$ ($M^{-1}.cm^{-1}$) ^a	λ_{em} ^b (nm)	Stokes shift (cm^{-1})	Φ_F ^c (%)
2	346	4.3	406	4271	0.10
	278	4.7			
3a	379 (sh)	4.2	406	1755	0.089
	363	6.0			
3b	285	5.6	407	1404	0.099
	385	4.1			
	366	4.9			
3c	295	5.3	407	875	0.06
	285	4.9			
	393	4.9			
	368	5.2			
	306	3.8			
4a	386	4.4	406	2842	0.11
	639	0.71			
	474	2.7			
	364	6.3			
4b	295	8.4	406	1616	0.05
	483	0.41			
	381	1.2			
	287	2.4			

^aRecorded in dichloromethane solvent, ^bExcited at $S_0 \rightarrow S_1$ absorption band. ^cDetermined by using 9, 10-diphenyl anthracene as standard ($\phi = 0.88$, in ethanol).

The emission spectra of ferrocenyl substituted pyrenes **2**, **3a – 3c**, **4a** and **4b** in dichloromethane are displayed in Figure 2. The characteristic emission pattern indicates the origin of emission from pyrene moiety. The emission wavelengths of ferrocenyl substituted pyrenes were found to be constant, but the quantum yield values were dependent on the nature of substituents. The quantum yield values follow the order **4a**>**2**>**3b**>**3a**>**3c**>**4b**. The fluorescence intensity increases upon addition of TCBD, in **4a** but decreases in **4b**, which can be explained on

the basis of the frontier molecular orbital (FMO) plots. The FMO plots reveal that the HOMO in **4a** is localized on pyrene, whereas in **4b** the HOMO is localized on ferrocene unit, which suggests that the fluorescence in **4b** is quenched due to fast non radiative deactivation of excited state due to photoinduced charge transfer from donor ferrocene to the acceptor TCBD unit (Figure 5).¹¹

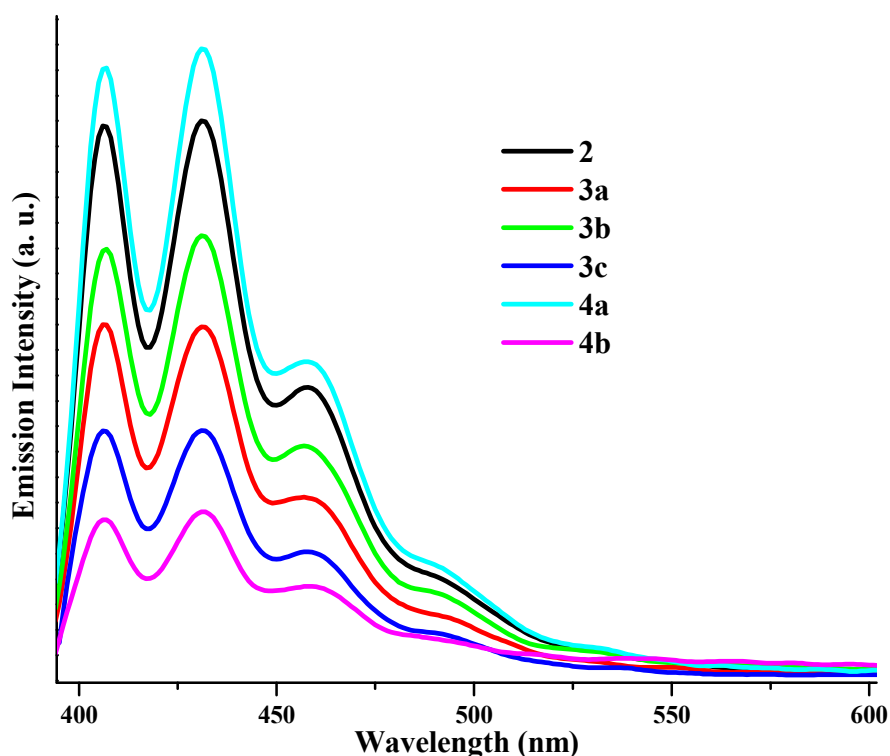


Figure 2. Emission spectra of ferrocenyl substituted pyrenes **2**, **3a** – **3c**, **4a** and **4b** in dichloromethane at the concentration of 0.1 optical densities.

ELECTROCHEMICAL PROPERTIES

The electrochemical properties of ferrocenyl substituted pyrenes **2**, **3a** – **3c**, **4a** and **4b** were investigated using cyclic and differential pulse voltammetric (CV and DPV) techniques in dichloromethane solvent using tetrabutylammoniumhexafluorophosphate (Bu_4NPF_6) as supporting electrolyte. The CV and DPV plots are shown in Figure 3 and Figure S2-S6 (ESI); and the corresponding data are listed in Table 2.

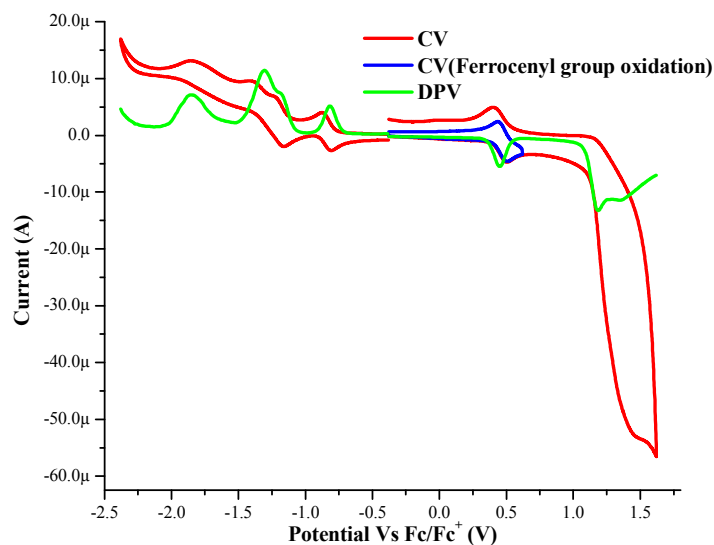


Figure 3. Overlaid CV and DPV plots of ferrocenyl substituted pyrene **4a**.

From the electrochemical data following observations are apparent: (a) The first oxidation (ferrocenyl oxidation) of **2** and **3a – 3c** appears at ~ 0.05 V. (b) The introduction of electron deficient TCBD unit increases the ferrocenyl oxidation of **4a** and **4b** to 0.45 and 0.07 V respectively, indicating strong interaction of ferrocene with TCBD in **4a** and weak interaction in **4b**. The *meta* linkage between ferrocene and TCBD hinders the electronic communication between ferrocene and TCBD in **4b** preventing the delocalization of ferrocenyl electrons to the TCBD. (c) The second oxidation potential of ferrocenyl substituted pyrenes **4a** and **4b** is higher than that of **2** and **3a – 3c** due to the introduction of electron deficient TCBD moiety. (d) The introduction of TCBD in **4a** and **4b** makes their reduction easier than **2** and **3a – 3c**. (e) The **4a** and **4b** exhibit two reduction waves corresponding to the reduction of two dicyanovinyl moieties. (f) The delocalization of ferrocenyl electrons to the TCBD makes it relatively electron rich in **4a**, which resulted the higher reduction potential of **4a** than **4b**. The *meta* linkage in **4b** hinders the delocalization electron density from ferrocene to the TCBD.

The computational calculations support the electrochemical studies. The HOMO of ferrocenyl substituted pyrene **4a** is localized on pyrene, whereas in **4b** it is localized on ferrocene (Figure 5). The

meta linkage in **4b** hinders the delocalization of ferrocenyl electrons to electron deficient TCBD which results the localization of HOMO on ferrocene. In case of **4a**, the delocalization of ferrocenyl electrons into the TCBD makes ferrocene electron deficient, leading to the localization of HOMO on relatively electron rich pyrene.

Table 2. The electrochemical properties of the ferrocenyl substituted pyrenes **2**, **3a – 3c**, **4a** and **4b**.^a

	E^4 Oxid ^b	E^3 Oxid ^b	E^2 Oxid ^b	E^1 Oxid (Fc)	E^1 Red	E^2 Red ^b	E^3 Red ^b	E^4 Red ^b
2	1.48	1.2	0.99	0.05	-1.32	-1.85		
3a	--	1.22	0.94	0.07	-1.31	-1.87		
3b	1.19	1.08	0.79	0.03	-1.31	-1.83		
3c	1.21	1.04	0.8	0.02	-1.34	-1.88		
4a		1.35	1.18	0.45	-0.82	-1.18	-1.31	-1.84
4b			1.15	0.08	-0.61	-1.12	-1.34	-1.82

^aThe electrochemical analysis was performed in a 0.1 M solution of Bu₄NPF₆ in dichloromethane at 100 mVs⁻¹ scan rate, versus Saturated Calomel Electrode (SCE) and referenced against Fc/Fc⁺, the potentials listed are half wave potentials. ^bIrreversible/quasi reversible wave.

COMPUTATIONAL CALCULATIONS

Computational calculations were performed using density functional theory at B3LYP/6-31G** level for C, H and N; and at Lanl2DZ level for Fe. The comparison of energy levels of ferrocenyl substituted pyrenes **3a**, and **3b** with **4a**, and **4b** are shown in Figure 4. The HOMO energy levels are stabilized in **4a** and **4b** than **3a** and **3b**. The better stabilization of HOMO in **4a** than **4b** supports the harder oxidation of **4a** than **4b**. Similarly the more stabilized LUMO in **4b** indicates the easier first reduction of **4b** than **4a**.

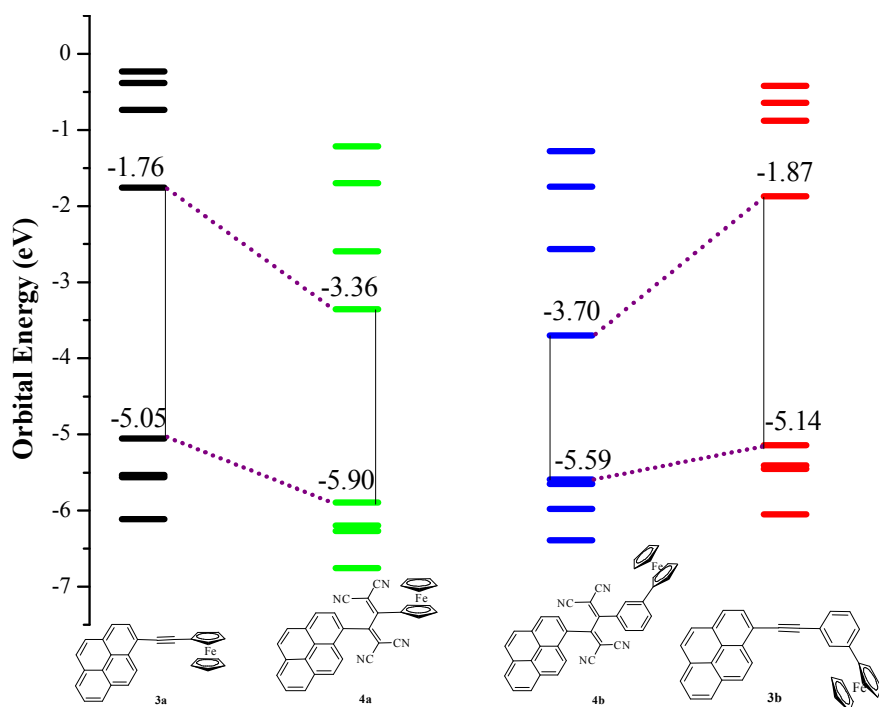


Figure 4. Comparison of computational energy levels of ferrocenyl substituted pyrenes **3a**, **3b** and **4a**, **4b**.

The frontier molecular orbital (FMO) plots and molecular electrostatic potential (MEP) diagram of ferrocenyl substituted pyrenes **2**, **3a** – **3c**, **4a** and **4b** are displayed in Figure 5. The LUMO of ferrocenyl substituted pyrenes **2** and **3a** – **3c** are located on the pyrene unit and spacer, whereas the LUMO of **4a** and **4b** is located on TCNE part, indicating strong acceptor nature of TCNE. In **4a** the HOMO is localized on pyrene unit, whereas in **4b** on ferrocene unit. The HOMO-LUMO distribution pattern indicates strong donor-acceptor interactions in **4a** and **4b**.

In the MEP diagrams the red color indicates higher electron density whereas the blue color indicates poor electron density. The MEP diagram reveals that the electron density of ferrocenyl substituted pyrenes **2** and **3a** – **3c** is distributed on the entire molecule, whereas in **4a** and **4b** it is accumulated on TCBD moiety (red color) due to its electron withdrawing nature. The comparison of MEP diagrams of **4a** and **4b** reveals that in **4b** the electron density is accumulated on TCBD and ferrocenyl part

also, whereas in case of **4a** the electron density is only on TCBD moiety. This supports the strong electronic communication of ferrocene with TCBD in **4a** and weak electronic communication in **4b**.

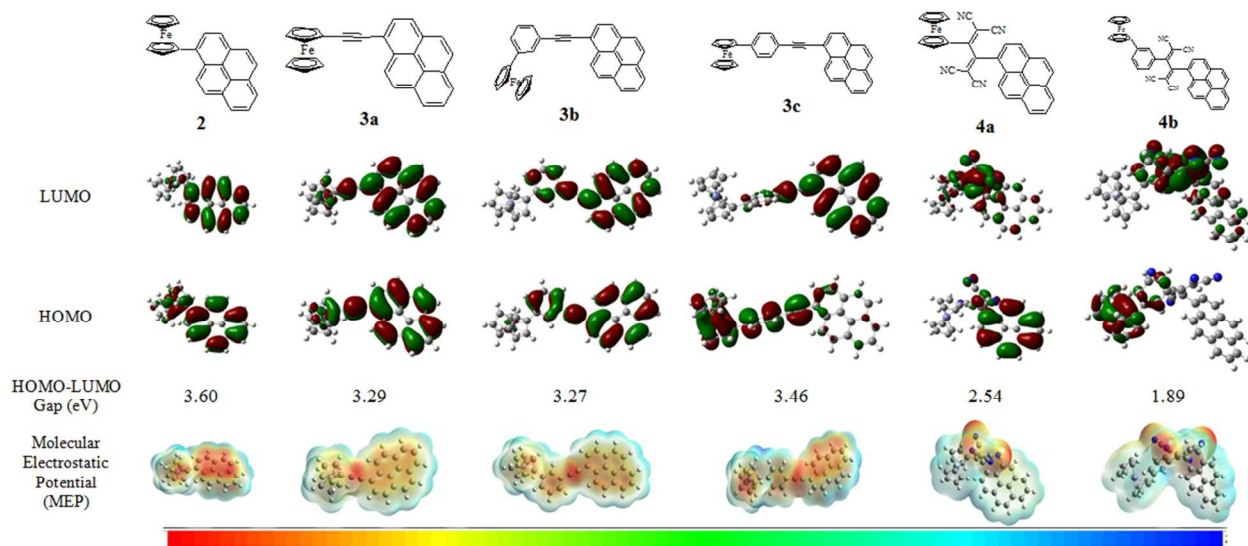


Figure 5. Frontier molecular orbitals and MEP diagrams of ferrocenyl substituted pyrenes **2**, **3a** – **3c**, **4a** and **4b** at the B3LYP/6-31G** level for C, H and N; and at the Lan12DZ level for Fe.

CRYSTAL STRUCTURE

The single crystal of ferrocenyl substituted pyrene **3b** was obtained by slow diffusion of hexane into the dichloromethane solution. The crystal data and structure refinement parameters are shown in Table S1 (ESI). The crystal structure shows slight variations from the energy optimized structure (Figure 6). The C≡C bond is slightly longer in the energy optimized structure than the crystal structure, and the C-C single bonds adjacent to C≡C are slightly shorter in energy optimized structure than crystal structure. The cyclopentadienyl ring of ferrocene is staggered in crystal structure with torsional angle of 24.53° whereas in energy optimized structure it is eclipsed (torsional angle = 0°). The slight variations in the crystal structure and energy optimized structure are may be due to the close packing of the crystal in the solid state.

Table 3. Distances of intermolecular interactions in the crystal structure of **3b**.

Interaction	Distance (Å)
C(26)-H(26)--- π C(30)	2.869
C(24)-H(24)--- π C(32)	3.262
C(22)-H(22)--- π C(26)	3.572

CONCLUSION

The ferrocenyl substituted pyrenes **2**, **3a** – **3c**, **4a** and **4b** were designed and synthesized using Suzuki and Sonogashira cross-coupling, and [2+2] cycloaddition-retroelectrocyclization reactions. The electronic absorption spectra of **2** and **3a** – **3c** show successive red shift with enhanced conjugation. The ferrocenyl substituted pyrene **4a** exhibits two strong charge transfer bands (from pyrene to TCBD and ferrocene to TCBD), on the other hand **4b** exhibits one strong charge transfer band (from pyrene to TCBD) and one weak charge transfer band (from ferrocene to TCBD). The spacer group between pyrene and ferrocene does not affect the emission wavelengths, whereas the quantum yield values are the function of spacers. The TCBD derivatives **4a** and **4b** show difficult oxidation and easier reduction. The ferrocenyl oxidation potential of **4a** is much higher than **4b**, due to better electronic communication. The photonic applications of these molecules are presently ongoing in our laboratory.

EXPERIMENTAL SECTION

General methods.

Chemicals were used as received unless otherwise indicated. All oxygen or moisture sensitive reactions were performed under nitrogen/argon atmosphere using standard schlenk method. ^1H NMR (400 MHz), and ^{13}C NMR (100MHz) spectra were recorded on the Bruker Avance (III) 400 MHz instrument, by using CDCl_3 as solvent. ^1H NMR chemical shifts are reported in parts per million (ppm) relative to the solvent residual peak (CDCl_3 , 7.26 ppm). Multiplicities are given as: s (singlet), d (doublet), t (triplet), q (quartet), dd (doublet of doublets), m (multiplet), and the coupling constants, J , are given in Hz. ^{13}C NMR chemical shifts are reported relative to the solvent residual peak (CDCl_3 , 77.36 ppm). UV-visible absorption spectra of all compounds were recorded on a Carry-100 Bio UV-visible Spectrophotometer. Fluorescence spectra of all the compounds were recorded on a Horiba Jobin Yvon Floromax 4P

spectrophotometer. Cyclic voltammograms (CVs) and Differential Pulse Voltammograms (DPVs) were recorded on a CHI620D electrochemical analyzer using Glassy carbon as working electrode, Pt wire as the counter electrode, and Saturated Calomel Electrode (SCE) as the reference electrode. The potentials were referenced against Fc/Fc^+ as per IUPAC guidelines.¹² HRMS was recorded on Bruker-Daltonics, micrOTOF-Q II mass spectrometer.

Synthesis and Characterization:

Procedure for Suzuki coupling reaction

Synthetic procedure for 1-ferrocenylpyrene (**2**): 1-Bromopyrene (200mg; 0.7117 mmol) and ferrocenyl boronic acid (196 mg; 0.8540 mmol) were dissolved in dry THF (22 mL) and 5ml 1M K_2CO_3 solution was added, the solution was degassed with argon and, the catalyst $\text{Pd}(\text{PPh}_3)_4$ (8.22mg; 0.007117 mmol) was added. The reaction mixture was stirred at 80° C for 24 h. After completion of reaction the solvent was removed under reduced pressure, and the residue was purified by column chromatography on (230–400 mesh size) silica with hexane: CH_2Cl_2 (4:1 ratio) and recrystallized from chloroform: hexane mixture to yield the desired product **2** as violet powder (181 mg, 0.47 mmol, yield: 68%).

Ferrocenyl substituted pyrene **2**

Crystalline solid. Yield: 70 % (192 mg); ^1H NMR (CDCl_3 , 400 MHz, ppm): δ 8.75 (d, 2H, $J = 8$ Hz), 8.41 (d, 2H, $J = 8$ Hz), 8.13-8.17 (m, 3H), 8.05 (t, 3H, $J = 4$ Hz), 7.98 (t, 1H, $J = 8$ Hz), 4.84 (t, 2H, $J = 2$ Hz), 4.49 (t, 2H, $J = 2$ Hz), 4.22 (s, 5H); ^{13}C NMR (CDCl_3 , 100 MHz, ppm):134.4, 132.0, 131.0, 130.2, 129.1, 129.0, 127.8, 127.3, 127.1, 126.3, 125.8, 125.3, 125.2, 124.9, 124.7, 87.6, 71.3, 70.1, 68.9; HRMS (ESI) $m/z =$ calculated for $\text{C}_{26}\text{H}_{18}\text{Fe} = 386.0753$, measured 386.0788.

Generalized procedure for Sonogashira coupling reaction

1-Bromopyrene (200mg; 0.7117 mmol) **1** and corresponding ferrocenyl alkyne (0.845 mmol) were dissolved in THF:triethylamine (10:1,v/v; 15 ml). The reaction mixture was purged with argon, and $\text{Pd}(\text{PPh}_3)_4$ (8.24 mg, 5 mol%), and CuI (5 mg, 5 mol%) were added, followed by stirring at 70 °C for 24 hours. Upon completion of reaction, the mixture was evaporated to dryness, and the crude product was

dissolved in CH_2Cl_2 , chromatographed on silica (1:1; hexanes: CHCl_3), and recrystallized from chloroform: hexane: ethanol (7:2:1) mixture to give **3a** – **3c** (yield 61-68%) as purple crystalline solid.

Ferrocenyl substituted pyrene **3a**

Crystalline solid. Yield: 68% (200 mg); ^1H NMR (δ): 8.63 (d, 2H, $J = 8$ Hz), 8.31-8.24 (m, 2H), 8.19-8.16 (m, 2H), 8.08-8.12 (d \times 2, 2H, $J = 8$ Hz), 8.01-8.06 (m, 2H), 4.68 (t, 2H, $J = 4$ Hz), 4.33-4.35 (m, 7H); ^{13}C NMR (CDCl_3 , 100 MHz, ppm): 132.1, 131.7, 131.5, 131.1, 129.8, 128.5, 128.2, 127.7, 126.6, 126.0, 125.78, 125.76, 124.95, 124.90, 124.8, 119.0, 94.7, 85.2, 72.0, 70.4, 69.4, 65.8; HRMS (ESI) $m/z =$ calculated for $\text{C}_{28}\text{H}_{18}\text{Fe} = 410.0753$, measured 410.0761.

Ferrocenyl substituted pyrene **3b**

Crystalline solid. Yield: 70% (243 mg); ^1H NMR (δ): 8.72 (d, 1H, $J = 8$ Hz), 8.21-8.27 (m, 4H), 8.10-8.16 (m, 2H), 8.02-8.07 (m, 2H), 7.83 (t, 1H, $J = 1.5$ Hz), 7.57-7.60 (dt, 1H, $J = 1.32$ Hz and 1.24 Hz), 7.52-7.55 (dt, 1H, $J = 1$ and 1.76 Hz) 7.37 (t, 1H, $J = 8.4$ Hz) 4.74 (t, 1H, $J = 2.04$ and 1.76 Hz), 4.37 (t, 1H, $J = 2$ and 1.76 Hz), 4.11 (s, 5H); ^{13}C NMR (CDCl_3 , 100 MHz, ppm): 140.2, 132.3, 131.6, 131.4, 130.0, 129.6, 129.3, 128.9, 128.7, 128.5, 127.6, 126.60, 126.57, 126.0, 125.9, 124.89, 124.86, 124.7, 123.8, 118.2, 95.7, 88.8, 84.7, 70.0, 70.0, 69.5, 66.9; HRMS (ESI) $m/z =$ calculated for $\text{C}_{34}\text{H}_{22}\text{Fe} = 486.1066$, measured 486.1070.

Ferrocenyl substituted pyrene **3c**

Crystalline solid. Yield: 61% (212 mg); ^1H NMR (δ): 8.77 (d, 1H, $J = 9$ Hz), 8.20-8.25 (m, 4H), 8.02-8.15 (m, 4H), 7.65 (d, 2H, $J = 8.2$ Hz), 7.53 (d, 2H, $J = 8.0$ Hz), 4.72 (s, 2H), 4.39 (s, 2H), 4.08 (s, 5H); HRMS (ESI) $m/z =$ calculated for $\text{C}_{34}\text{H}_{22}\text{Fe} = 486.1066$, measured 486.1101.

Procedure for the synthesis of ferrocenyl substituted pyrene 4a by [2+2] cycloaddition-retroelectrocyclization reaction-

TCNE (31 mg, 0.24 mmol) was added to a solution of **3a** (100 mg, 0.24 mmol) in dichloromethane (20 mL) under argon atmosphere. The reaction mixture was stirred for 6 h at room temperature. After completion of reaction the solvent was removed under reduced pressure, and the product was purified by

column chromatography with dichloromethane as eluent to yield **4a** as dark colored solid. Yield: 80% (105 mg).

Ferrocenyl substituted pyrene **4a**

Crystalline solid. Yield: 80% (105 mg); ^1H NMR (δ): 8.49 (d, 1H, $J = 9.28$ Hz), 8.36-8.41 (m, 2H), 8.22-8.30 (m, 2H), 8.11-8.18 (m, 2H), 7.94 (d, 1H, $J = 8.28$ Hz), 5.23 (s, 1H), 4.89 (s, 2H), 4.77 (s, 2H), 4.33 (s, 5H); ^{13}C NMR (CDCl_3 , 100 MHz, ppm): 135.3, 131.6, 131.5, 130.7, 128.2, 127.9, 127.7, 127.4, 126.1, 125.8, 125.1, 124.6, 123.4, 115.8, 114.5, 112.2, 111.9, 103.7, 95.7, 92.4, 90.7, 86.5, 76.0, 75.8, 75.5, 73.1, 73.0, 72.8, 72.6, 72.1; HRMS (ESI) m/z = calculated for $\text{C}_{34}\text{H}_{18}\text{N}_4\text{Fe}$ = 477.0513, measured 477.0474.

Procedure for the synthesis of ferrocenyl substituted pyrene **4b** by [2+2] cycloaddition-retroelectrocyclization reaction-

TCNE (26 mg, 0.21 mmol) was added to a solution of **3b** (100 mg, 0.21 mmol) in 1,2-dichloroethane and acetonitrile (1:1) solvent mixture (20 mL) under argon atmosphere. The reaction mixture was refluxed for 72 hours at 140 °C temperature. After completion of reaction the solvents were removed under reduced pressure, and the product was purified by column chromatography with dichloromethane as eluent to yield **4b** as dark colored solid. Yield: 85 % (107 mg).

Ferrocenyl substituted pyrene **4b**

Crystalline solid. Yield: 85% (107 mg);

^1H NMR (δ): 8.35-8.42 (m, 3H), 8.29 (d, 1H, $J = 8.76$ Hz), 8.24 (d, 1H, $J = 8.28$ Hz), 8.11-8.17 (m, 3H), 7.92 (d, 1H, $J = 8.04$ Hz), 7.7 (bs, 1H), 7.61-7.63 (m, 1H), 7.3-7.4 (m, 2H), 5.54 (t, 2H, $J = 1.76$ Hz), 4.32 (t, 2H, $J = 1.76$ Hz), 3.92 (s, 5H); HRMS (ESI) m/z = calculated for $\text{C}_{40}\text{H}_{22}\text{N}_4\text{Fe}$ = 614.1189, measured 614.1160.

ASSOCIATED CONTENT

Supporting Information

† Electronic supplementary information (ESI) available: General experimental methods, electrochemical data, theoretical calculations, crystal structure data and copies of ^1H , ^{13}C NMR and HRMS spectra of new

compounds. CCDC 1054932 contains crystal structure of **3b**. For ESI and crystallographic data in CIF electronic format see DOI: 10.1039/b000000x/

AUTHOR INFORMATION

Corresponding Author

*E-mail: rajneeshmisra@iiti.ac.in; Fax: +91 731 2361 482; Tel: +91 731 2438 710

ACKNOWLEDGMENTS

RM thanks CSIR, and DST, New Delhi for financial support. BD and TJ thank CSIR and UGC, New Delhi respectively for their fellowships. We are thankful to Sophisticated Instrumentation Centre (SIC), IIT Indore.

¹ (a) C. Joachim, J. K. Gimzewski and A. Aviram, *Nature*, 2000, **408**, 541–548; (b) A. R. Pease, J. O. Jeppesen, J. F. Stoddart, Y. Luo, C. P. Collier and J. R. Heath, *Acc. Chem. Res.*, 2001, **34**, 433–444; (c) R. F. Service, *Science*, 2001, **293**, 782–785; (d) M. Ruben, J. M. Lehn and P. Muller, *Chem. Soc. Rev.*, 2006, **35**, 1056–1067; (f) G. S. He, L. S. Tan, Q. Zheng and P. N. Prasad, *Chem. Rev.*, 2008, **108**, 1245–1330; (e) M. Liangwab and J. Chen, *Chem. Soc. Rev.*, 2013, **42**, 3453–3488; (f) K. Szaciłowski, *Chem. Rev.* 2008, **108**, 3481–3548; (g) J. C. May, J. H. Lim, I. Biaggio, N. N. P. Moonen, T. Michinobu and F. Diederich, *Opt. Lett.*, 2005, **30**, 3057–3059.

² (a) Q. T. Zhang and J. M. Tour, *J. Am. Chem. Soc.*, 1998, **120**, 5355–5362; (b) J. L. Wang, Q. Xiao and J. Pei, *Org. Lett.*, 2010, **12**, 4164–4167; (c) T. Tanaka and A. Osuka, *Chem. Soc. Rev.*, 2015, **44**, 943–969; (d) H. L. Dong, H. F. Zhu, Q. Meng, X. Gong and W. P. Hu, *Chem. Soc. Rev.*, 2012, **41**, 1754–1808; (e) B. Dhokale, T. Jadhav, S. M. Mobin and R. Misra, *Chem. Commun.*, 2014, **50**, 9119–9121; (f) R. Misra, T. Jadhav, B. Dhokale, P. Gautam, R. Sharma, R. Maragani and S. M. Mobin, *Dalton Trans.*, 2014, **43**, 13076–13086; (g) R. Misra, B. Dhokale, T. Jadhav and S. M. Mobin, *Dalton Trans.*, 2014, **43**, 4854.

³ (a) Y. O. Lee, T. Pradhan, S. Yoo, T. H. Kim, J. Kim and J. S. Kim, *J. Org. Chem.*, 2012, **77**, 11007; (b) T. M. Figueira-Duarte, K. Mullen, *Chem. Rev.*, 2011, **111**, 7260–7314.

⁴ (a) S. W. Yang, A. Elangovan, K. C. Hwang and T. I. Ho, *J. Phys. Chem. B*, 2005, **109**, 16628–16635; (b) C. Lambert, J. Ehbets, D. Rausch and M. Steeger, *J. Org. Chem.* 2012, **77**, 6147–6154.

⁵ (a) P. L. Pauson, *Q. Chem. Soc. Rev.*, 1955, **9**, 391–414; (b) H. Nishihara, *Adv. Inorg. Chem.*, 2002, **53**, 41–86; (c) D. R. Van Staveren and N. M. Nolte, *Chem. Rev.*, 2004, **104**, 5931–5985; (d) R. C. J. Atkinson, V. C. Gibson and N. J. Long, *Chem. Soc. Rev.*, 2004, **33**, 313–328; (e) R. Misra, R. Maragani, T. Jadhav and S. M. Mobin, *New J. Chem.*, 2014, **38**, 1446–1457; (f) A. Vecchi, P. Galloni, B. Floris, S. V. Dudkin and V. N. Nemykin, *Coordination Chem. Rev.*, 2015,

<http://dx.doi.org/10.1016/j.ccr.2015.02.005>; (g) C. J. Ziegler, K. Chanawanno, A. Hasheminsasab, Y. V. Zatsikha, E. Maligaspe and V. N. Nemykin, *Inorg. Chem.* 2014, DOI: dx.doi.org/10.1021/ic500526k; (h) X. Yin, Y. Li, Y. Zhu, X. Jing, Y. Li and D. Zhu, *Dalton Trans.*, 2010, **39**, 9929-9935; (i) Y. Li, T. Liu, H. Liu, M. Z. Tian, Y. Li, Y. *Acc. Chem. Res.*, 2014, **47**, 1186–1198.

⁶ (a) B. Dhokale, P. Gautam, S. M. Mobin and R. Misra, *Dalton Trans.*, 2013, **42**, 1512-1518; (b) P. Gautam, B. Dhokale, S. M. Mobin and R. Misra, *RSC Adv.*, 2012, **2**, 12105-12107; (c) R. Misra, B. Dhokale, T. Jadhav and S. M. Mobin, *Dalton Trans.*, 2014, **43**, 4854; (d) R. Misra, B. Dhokale, T. Jadhav and S. M. Mobin, *Organometallics*, 2014, **33**, 1867–1877; (e) R. Misra, B. Dhokale, T. Jadhav and S. M. Mobin, *New J. Chem.* **2014**, *38*, 3579-3585; (f) R. Misra and P. Gautam, *Org. Biomol. Chem.*, 2014, **12**, 5448-5457; (g) R. Misra, R. Maragani, P. Gautam and S. M. Mobin, *Tetrahedron Lett.*, 2014, **55**, 7102–7105; (h) R. Misra, P. Gautam and R. Maragani, *Tetrahedron Lett.*, 2014, *56*, 1664–1666; (i) B. Dhokale, T. Jadhav, S. M. Mobin, and R. Misra, *Dalton Trans.*, 2015, DOI: 10.1039/C5DT00565E.

⁷ (a) T. M. Figueira-Duarte and K. Mullen, *Chem. Rev.*, 2011, **111**, 7260–7314; (b) S. I. Kirin, H. B. Kraatz and N. M. Nolte, *Chem. Soc. Rev.*, 2006, *35*, 348–354.

⁸ (a) L. Cuffe, R. D. A. Hudson, J. F. Gallagher, S. Jennings, C. J. McAdam, R. B. T. Connelly, A. R. Manning, B. H. Robinson and J. Simpson, *Organometallics*, **2005**, *24*, 2051; (b) M. D. Gonzalez, F. Oton, R. A. Orenes, A. Espinosa, A. Tárraga and P. Molina, *Organometallics*, 2014, **33**, 2837–2852; (c) R. Martinez, A. I. Ratera, A. Tarraga, P. Molina and J. Veciana, *Chem. Commun.*, 2006, 3809–3811; (d) M. Kaur, P. Kaur, V. Dhuna, S. Singh and K. Singh, *Dalton Trans.*, 2014, **43**, 5707–5712; (e) T. Romero, A. Caballero, A. Tarraga and P. Molina, *Org. Lett.*, 2009, **11**, 3466–3469.

⁹ (a) M. Kivala, C. Boudon, J.-P. Gisselbrecht, P. Seiler, M. Gross and F. Diederich, *Angew. Chem.*, 2007, **119**, 6473–6477; M. Kivala, C. Boudon, J.-P. Gisselbrecht, P. Seiler, M. Gross and F. Diederich, *Angew. Chem., Int. Ed.*, 2007, **46**, 6357–6360; (b) M. Kivala, T. Stanoeva, T. Michinobu, B. Frank, G. Gescheidt and F. Diederich, *Chem.–Eur. J.*, 2008, **14**, 7638–7647; (c) B. B. Frank, B. C. Blanco, S. Jakob, F. Ferroni, S. Pieraccini, A. Ferrarini, C. Boudon, J.-P. Gisselbrecht, P. Seiler, G. P. Spada and F. Diederich, *Chem.–Eur. J.*, 2009, **15**, 9005–9016; (d) M. Yamada, P. Rivera-Fuentes, W. B. Schweizer and F. Diederich, *Angew. Chem., Int. Ed.*, 2010, **49**, 3532–3535; (e) T. Shoji, A. Maruyama, C. Yaku, N. Kamata, S. Ito, T. Okujima and K. Toyota, *Chem. Eur. J.*, 2015, **21**, 402–409; (f) T. Michinobu, *Chem. Soc. Rev.*, 2011, **40**, 2306–2316; (g) T. Shoji, S. Ito, K. Toyota, M. Yasunami and N. Morita, *Chem.–Eur. J.*, 2008, **14**, 8398–8408; (h) M. Morimoto, K. Murata and T. Michinobu, *Chem. Commun.*, 2011, **47**, 9819–9821; (i) T. M. Pappenfus, D. K. Schneiderman, J. Casado, J. T. L. Navarrete, M. C. R. Delgado, G. Zotti, B. Vercelli, M. D. Lovander, L. M. Hinkle, J. N. Bohnsack and K. R. Mann, *Chem. Mater.*, 2011, **23**, 823–831; (j) Y. Hua, J. He, C. Zhang, C. Qin, L. Han, J. Zhao, T. Chen, W. Y.

Wong, W. K. Wong and X. Zhu, *J. Mater. Chem. A*, 2015, DOI: 10.1039/C4TA05350H; (k) W. Y. Wong, *Dalton Trans.*, 2007, 4495–4510.

10 (a) T. Mochida and S. Yamazaki, *J. Chem. Soc. Dalton Trans.* 2002, 3559–3564; (b) T. Shoji, S. Ito, T. Okujima and N. Morita, *Chem. Eur. J.*, 2013, **19**, 5721–5730.

11 (a) B. Dhokale, P. Gautam and R. Misra, *Tetrahedron Lett.*, 2012, **53**, 2352-2354; (b) T. Jadhav, R. Maragani, R. Misra, V. Sreeramulu, D. N. Rao and S. M. Mobin, *Dalton Trans.*, 2013, **42**, 4340-4342; (c) R. Sharma, R. Maragani, S. M. Mobin and R. Misra, *RSC Adv.*, 2013, **3**, 5785; (d) R. Misra, T. Jadhav and S. M. Mobin, *Dalton Trans.*, 2013, **42**, 16614-16620; (e) R. Maragani and R. Misra, *Tetrahedron Lett.*, 2013, **54**, 5399–5402; (f) R. Misra, T. Jadhav and S. M. Mobin, *Dalton Trans.*, 2014, **43**, 2013-2022; (g) R. Misra, R. Sharma and S. M. Mobin, *Dalton Trans.*, 2014, **43**, 6891-6896; (h) V. A. Nadtochenko, N. N. Denisov, V. Y. Gak, N. V. Abramova and Loim, N. M. *Russ. Chem. Bull.*, 1999, **48**, 1900; (i) S. Barlow and S. R. Marder, *Chem. Commun.*, 2000, 1555-1562.

12 G. Gritzner, G. Kuta, *J. Pure Appl. Chem.*, 1984, **56**, 461-466.